Journal of Molecular Catalysis A: Chemical 302 (2009) 20–27

Contents lists available at ScienceDirect

Journal of Molecular Catalysis A: Chemical

journal homepage: www.elsevier.com/locate/molcata

Dimethyl ether synthesis on the admixed catalysts of Cu-Zn-Al-M (M = Ga, La, Y, Zr) and γ-Al_2O_3: The role of modifier

Akula Venugopal[a,*], Jelliarko Palgunadi[b], Jung Kwang Deog[b,**], Oh-Shim Joo[b], Chae-Ho Shin[c]

[a] Catalysis & Physical Chemistry, Indian Institute of Chemical Technology, Tarnaka, Hyderabad 500 607, India
[b] Hydrogen Energy Research Center, Korea Institute of Science and Technology, Cheongryang P.O. Box 131, Seoul, Republic of Korea
[c] Department of Chemical Engineering, Chungbuk National University, Cheongju, Chungbuk 361-763, Republic of Korea

ARTICLE INFO

Article history:
Received 10 June 2008
Received in revised form
10 November 2008
Accepted 24 November 2008
Available online 9 December 2008

Keywords:
Hydrotalcite-like structure
Methanol synthesis
DME synthesis
Methanol dehydration
Cu based catalysts

ABSTRACT

Dimethyl ether synthesis has been conducted on the admixed catalysts of Cu based catalysts (for methanol synthesis) and γ-Al_2O_3 (for methanol dehydration). The Cu-Zn-Al-M (M = Ga, La, Y, Zr) hydrotalcite-like structures as catalyst precursors for methanol synthesis part of the admixed catalysts are synthesized by the co-precipitation method. The physico-chemical characteristics of the catalysts are analyzed by BET-surface area, XRD, TPR, SEM/EDS, XPS and N_2O pulse chemisorption studies. DME synthesis experiments showed that the CO conversion and DME yield are linearly correlated with Cu metal surface areas of Cu based catalysts admixed with γ-Al_2O_3, indicating that methanol synthesis rate can control the overall DME synthesis rate. The yttrium-modified Cu-Zn-Al admixed catalysts showed the superior activity with a DME yield of 47.7% to other Cu-based catalysts. The reason may be attributed to the increase in Cu metal surface area by the addition of yttrium.

1. Introduction

Synthesis of dimethyl ether (DME) using syngas has been a topic of interest in recent times due to the growing demand for petroleum products and diminution of the existing fossil fuels. DME can be produced on the admixed catalysts of Cu-Zn-Al and solid acid catalysts in a single step. The principal DME synthesis is mainly composed of methanol synthesis, methanol dehydration and water gas shift reaction.

$CO + 2H_2 \leftrightarrow CH_3OH$ Methanol synthesis

$2CH_3OH \leftrightarrow CH_3OCH_3 + H_2O$ Methanol dehydration

$CO + H_2O \leftrightarrow CO_2 + H_2$ Water gas shift reaction

Some authors tried to prepare bifunctional catalysts that cause both methanol synthesis and methanol dehydration to produce DME [1–2], while others used the physically admixed catalysts of methanol synthesis (Cu/ZnO based catalysts) and methanol dehydration catalysts (solid acid catalysts) [3–5]. However, the advantages of the bifunctional catalysts over the admixed catalysts are not clear.

DME synthesis on the admixed catalysts of Cu/Zn/Al_2O_3 and different solid acid catalysts showed similar activities, suggesting that DME synthesis would not be dependent on the acidity of the solid acid catalysts [6]. On the contrary, it is reported that the rate of DME direct synthesis is determined by the acid properties of the solid acid catalysts [7].

Methanol synthesis catalysts have been conventionally prepared by a co-precipitation method. It is known that precursors of Cu-Zn-Al hydrotalcite-like (HTlc) structures generate small clusters of Cu, the active species for the conversion of syngas to methanol [8]. The evolution of active copper particles and their dispersion depend on the preparation conditions, Cu/Zn mole ratio, pH and heat treatments during and after the precipitation [9–11]. The conversion of syngas to methanol is dependent upon the copper metal surface area and finely dispersed copper can be obtained through the precursors of ternary Cu-Zn-Al hydrotalcite structures prepared by a co-precipitation method and subsequent thermal decomposition. It is a known fact that high copper dispersion leads to higher methanol rates [8,12].

Another aspect is that the introduction of small amounts of tri- and tetra-valent metal ions into Cu-ZnO matrix enables the formation of cationic defects in the catalyst structure and these cationic defects enrich and stabilize copper on the surface of Cu based catalysts for methanol synthesis during reduction and reaction [13].

* Corresponding author. Tel.: +91 40 27193510; fax: +91 40 27160921.
** Corresponding author. Tel.: +82 2 958 5218; fax: +82 2 958 5219.
E-mail addresses: akula@iict.res.in (A. Venugopal), jkdcat@kist.re.kr (J.K. Deog).

1381-1169/$ – see front matter © 2008 Elsevier B.V. All rights reserved.
doi:10.1016/j.molcata.2008.11.038

In the present study the Cu-Zn-Al-M (M = Ga, La, Y and Zr) catalysts are prepared and characterized in order to study the effect of metal cation on copper metal surface area and in order to clarify the role of methanol synthesis catalysts for a single-step DME synthesis. The reason for choosing Ga-, La-, Y- and Zr-modified Cu-Zn-Al catalysts is to enhance the methanol synthesis rates since these particular promoters would enhance the CO conversion rates at low temperatures, consequently higher DME yields could be obtained in the presence of a solid acid catalyst. The activity of the admixture of Cu-Zn-Al-M catalysts and γ-Al_2O_3 for DME synthesis has been correlated to the copper metal surface areas of the catalysts.

2. Experimental

2.1. Catalyst preparation

Catalyst precursors were prepared by the co-precipitation method with mol.% ratios of Cu:Zn:Al = 6:3:1 (designated as CZA) and Cu:Zn:Al:M = 6:2.5:1:0.5 (designated with respect to the metal used, i.e. M = Ga, La, Y, and Zr). About 0.6 l aqueous solution of $Cu(NO_3)_2$ $6H_2O$, $Zn(NO_3)_2$ $6H_2O$, $Al(NO_3)_3$ $9H_2O$, and if necessary, $Ga(NO_3)_3$ $6H_2O$, $La(NO_3)_3$ $6H_2O$, $Y(NO_3)_3$ $6H_2O$, or $ZrO(NO_3)_4$ $6H_2O$ (solution A) and a solution B containing 2 M NaOH and 1 M Na_2CO_3 (1:1 = v/v) were added simultaneously to 2.0 l distilled water under vigorous stirring. The rate of addition of solution A was approximately 0.5 l/h with a constant pH ~7.0 ± 0.1 maintained by adjusting the flows of solutions A and B. The co-precipitation was carried out at room temperature and subsequently the precipitate was kept at 70 °C for 1 h, and washed several times until the pH of the gel reached the pH of the distilled water that had been used for the preparation. The residual Na content is found to be <0.03% as measured by atomic absorption spectroscopy. The precipitate was filtered, oven dried at 100 °C for 24 h and calcined in static air at 400 °C for 3 h. For simplicity the samples are designated as for example CZAGa for Cu-Zn-Al-Ga catalyst and similarly named for the rest of the samples corresponding to their modified metals.

2.2. Characterization

The BET-surface areas of the calcined catalysts were obtained by means of dinitrogen physisorption at ca. −196 °C using a Micromeritics ASAP 2000 instrument. Prior to the measurements the catalysts were degassed at 120 °C for 0.5 h. The X-ray diffraction analysis of the oven dried, calcined and used catalysts was carried out in the 2θ range from 5 to 90° using a Rigaku diffractometer employing Ni filtered Cu Kα radiation at 40 kV and 126 mA. The XRD patterns were compared with ICDD data. The temperature programmed reduction (TPR) and the N_2O titration were carried out by using a tubular reactor system connected to a thermal conductivity unit. In the case of N_2O titrations a Porapak N column was used for the N_2O and N_2 separation and estimations. In a typical experiment about 30–80 mg of catalyst was loaded and reduced in 5% H_2/Ar stream at 250 °C for 1 h and the reactor was purged in a He stream at 250 °C for 0.5 h and cooled down to 90 °C at which the N_2O titrations were carried out. Several replicate experiments were carried out and the Cu metal surface areas were measured so that the N_2O titration takes place in a single pulse. In this investigation a surface copper density of 1.46×10^{19} atoms/m^2 and the adsorption stoichiometry of Cu:O = 2:1 were taken into consideration for the copper metal area measurements [14]. For TPR analysis 5% dihydrogen in Ar was used. The scanning electron microscopy (SEM) and energy dispersive spectroscopy (EDS) analysis are performed by a Hitachi FE-SEM S—400 microscope at an accelerating voltage 0.5–30 kV. X-ray photoelectron spectroscopic (XPS) measurements were performed on a VG Scientific ESCA LAB 210 spectrometer with a Mg Kα X-ray source (1253.6 eV). The pressure inside the analysis chamber was typically maintained at lower than 5×10^{-10} torr. The recorded spectra were always fitted by using Gauss–Lorentz curves. All the binding energies were referenced to the C 1s line at 284.6 eV from adventitious carbon. The binding energy values reported here were within an accuracy of ±0.3 eV.

2.3. Activity measurements

DME synthesis was carried out in a fixed bed micro reactor (O.D.: 0.95 cm, length: 30 cm) loaded with 1.0 g of catalyst composed of 0.5 g of activated methanol synthesis catalyst and 0.5 g of methanol dehydration catalyst, i.e. γ-Al_2O_3. Prior to the reaction the catalysts were reduced in a stream of 5% H_2/Ar in sequential reduction steps as follows: 1st step: treatment at 100 °C/0.5 h, 2nd step: reduction at 180 °C/0.5 h, 3rd step: reduction at 240 °C/2 h and 4th step: reduction at 280 °C/0.5 h. The reaction was conducted under the conditions of a H_2 to CO ratio of 1.5, a GHSV of 6000 to 12,000 h^{-1}, a pressure of 600 psig and a reaction temperature ranging from 250 to 280 °C. The pressure was maintained by means of a back-pressure regulator and the gas flow rates were controlled by mass flow controllers. The reaction mixture was passed through a purifier in order to eliminate the traces of water, oxygen and iron carbonyl that would deactivate the catalyst. Then, the noticeable activity loss was not observed during the data collection of 1 day. The effluent gas mixture was analyzed by an on-line gas chromatograph equipped with a thermal conductivity detector using Porapak Q (2 m) and Carbosphere (0.3 m) columns in series. The experimental error in the evaluation of the catalysts was found to be ±2% unless otherwise mentioned.

3. Results and discussion

3.1. BET-surface area and XRD

The XRD patterns of the oven dried and calcined samples are displayed in Figs. 1 and 2, respectively and the corresponding phases are presented in Table 1. The BET-surface areas, Cu metal surface areas by N_2O titration, particle sizes by SEM analysis, the CO conversion and DME yields with the Cu-Zn-Al and Cu-Zn-Al-M (M = Ga, La, Y, Zr) catalysts are presented in Table 2. The yttrium-modified Cu-Zn-Al catalyst possesses extremely high specific surface area over the other catalysts. The XRD analysis of the oven-dried samples

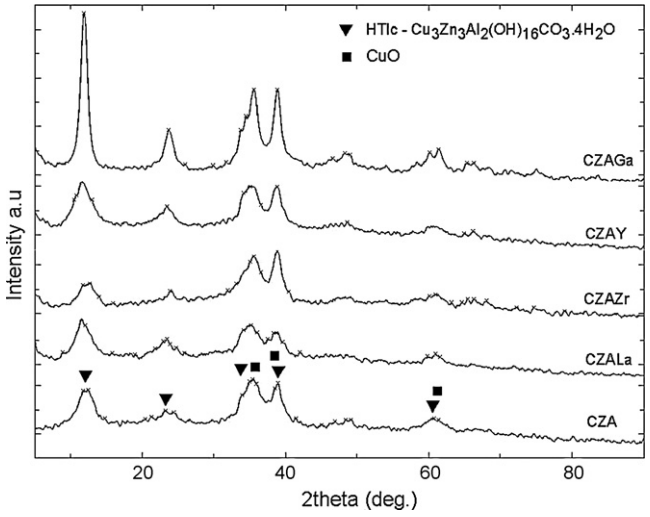

Fig. 1. The XRD patterns of the oven dried Cu-Zn-Al and Cu-Zn-Al-M (M = Ga, La, Y and Zr) catalysts.

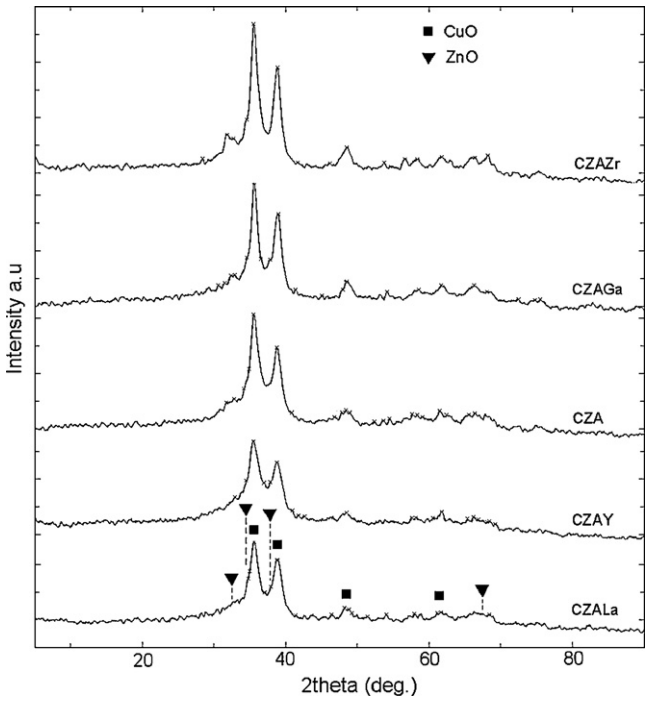

Fig. 2. The XRD patterns of the calcined Cu-Zn-Al and Cu-Zn-Al-M (M = Ga, La, Y and Zr) catalysts.

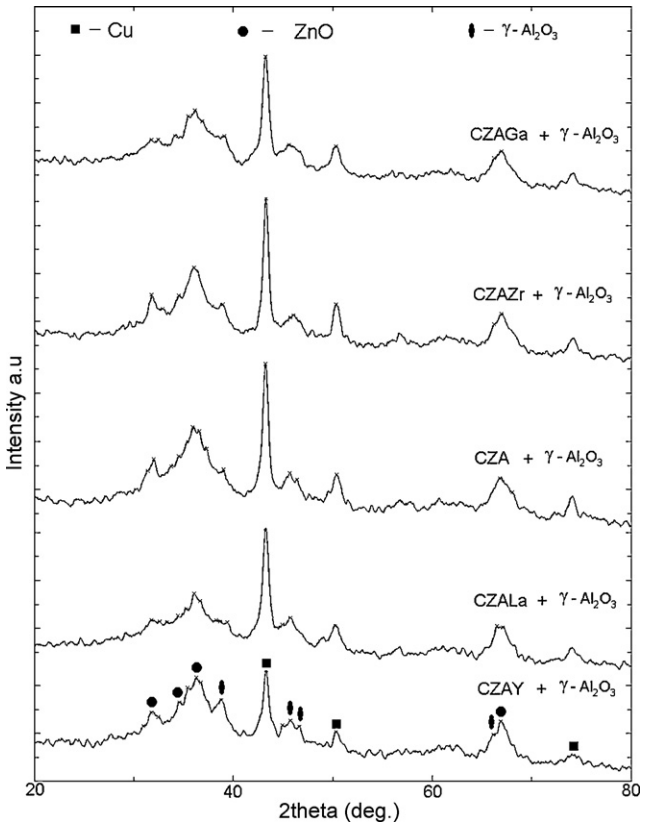

Fig. 3. : XRD patterns of the used admixed catalysts of Cu-based catalysts (Cu-Zn-Al or Cu-Zn-Al-M) and γ-Al_2O_3 catalysts.

revealed the presence of the hydrotalcite structure attributed to the $Cu_3Zn_3Al_2(OH)_{16}{\cdot}4H_2O$ phase (Fig. 1). The reflections appeared at 2θ = 11.8, 23.7, 34.7, 39.4, 47.1, 53.3, and 37.4° and the corresponding "*d*" values of 0.749, 0.373, 0.257, 0.228, 0.192, 0.171, and 0.239 nm indicate the presence of the $Cu_3Zn_3Al_2(OH)_{16}{\cdot}4H_2O$ phase. The diffraction lines due to the HTlc phase are broad except the Cu-Zn-Al-Ga catalyst wherein sharp peaks are observed. Very weak diffraction lines due to the CuO phase are also noticed in all the oven-dried samples which can be ascribed to behavior of Cu^{2+} when the Cu^{2+}/Zn^{2+} ratio is higher than 1; formation of CuO along with hydrotalcite occurs due to the Jahn–Teller effect [15]. The EDS analysis of these samples (Table 1) indicates the Cu/Zn ratios higher than 1 in all the case, which is in good agreement with the occurrence of the CuO phase in oven-dried samples.

It is observed (Fig. 2) that upon thermal decomposition at 400 °C for 4 h the HTlc structure collapses to form predominantly the CuO phase (2θ = 35.7, 38.9° ICDD: 45-0937) and very weak reflections due to the ZnO (2θ = 36.2, 31.8° ICDD: 89-0511) phase and the CuO and ZnO peaks are not finely resolved. The broad reflections indicate that part of Cu may be dissolved in the Zn matrix or the CuO

Table 1
The physical characteristics and nominal compositions of the Cu-Zn-Al-M (M = Ga, La, Y and Zr) oxide catalysts obtained from EDS analysis.

Catalyst	Oven dried	Calcined	Cu (mol.%)	Zn (mol.%)	Al (mol.%)	M (mol.%)	Cu/Zn
CZA	[b]HTlc, [a]CuO	[a]CuO, [c]ZnO	58.6	30.0	10.9	–	1.95
CZAGa	[a]HTlc, [b]CuO	[a]CuO, [d]ZnO	58.8	25.9	11.2	3.9	2.27
CZALa	[a]HTlc, [b]CuO	[a]CuO, [c]ZnO	60.7	24.8	10.4	4.1	2.44
CZAY	[a]HTlc, [b]CuO	[a]CuO, [d]ZnO	58.8	25.2	10.8	4.2	2.33
CZAZr	[b]HTlc, [a]CuO	[a]CuO, [d]ZnO	59.0	26.0	10.3	4.6	2.26

ICDD: HTlc—37-0629, CuO: 45-0937, ZnO-ICDD: 89-0511.
[a] Major.
[b] Minor.
[c] Weak.
[d] Very weak.

Table 2
The chemical characteristics of the Cu-Zn-Al and Cu-Zn-Al-M (M = Ga, La, Y and Zr) catalysts.

Catalyst	S_{BET} (m^2/g)	Cu metal surface area (m^2/g)	Average particle size (nm)[a]	CO conversion at 250 °C	%DME yield at 250 °C
CZA	57	8.0	69.1	50.5	33.3
CZAGa	51	1.4	100.8	28.7	19.5
CZALa	78	5.7	78.0	31.3	21.0
CZAY	114	11.7	54.7	59.5	40.3
CZAZr	85	6.9	67.3	35.8	23.8

[a] The average particle size measured from SEM analyses.

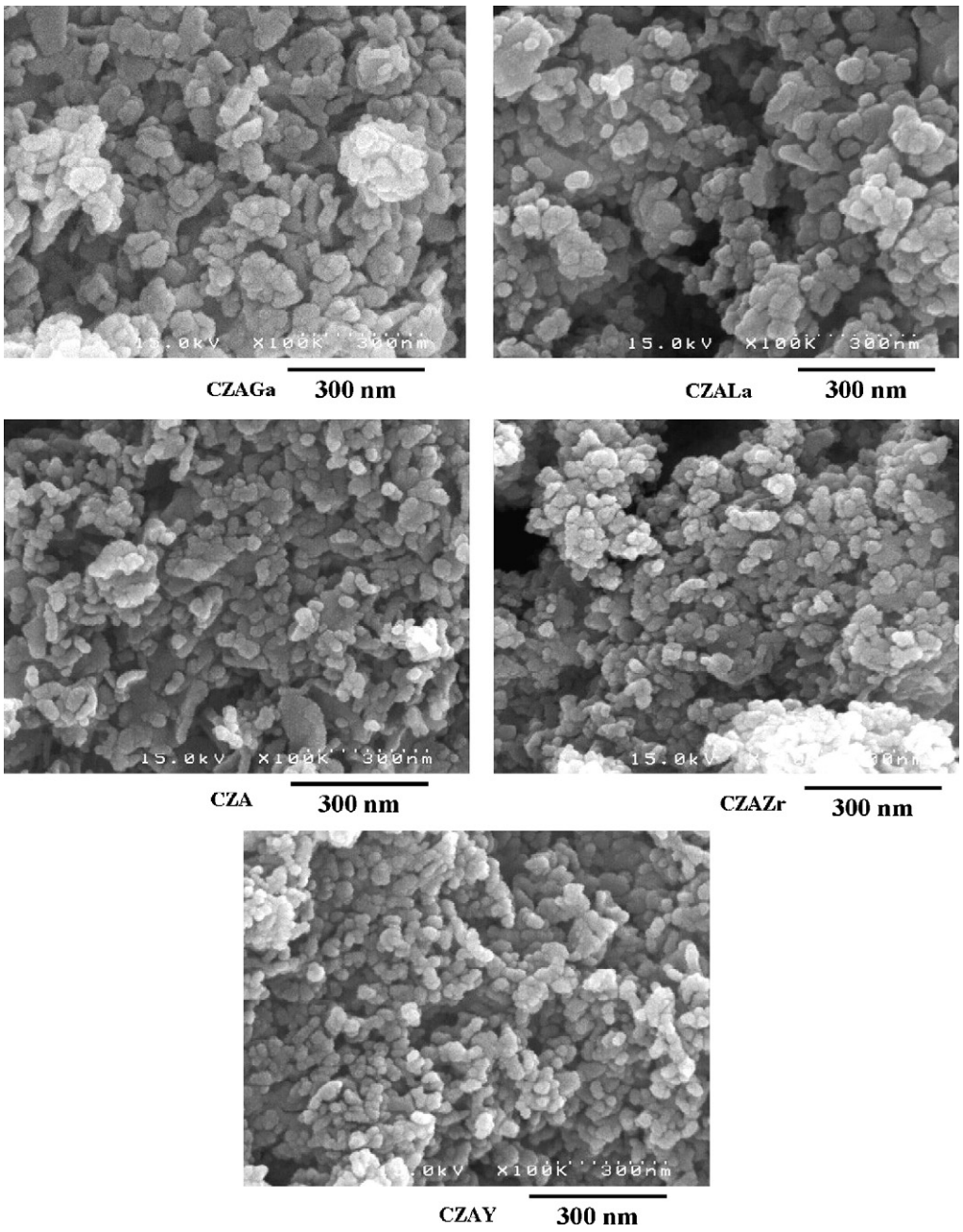

Fig. 4. The SEM images of the Cu-Zn-Al and Cu-Zn-Al-M (M = Ga, La, Y and Zr) catalysts.

phase is in intimate contact with the ZnO phase [16]. Reflections due to Al_2O_3 and any of the M_xO_y (M = Ga, La, Y and Zr) phases could not be observed in the calcined form. This is due to the fact that these elements are present in small quantities and may be in the amorphous state or might be due to low calcination temperature, i.e. 400 °C at which formation of these metal oxide crystalline species is improbable.

The XRD patterns of the admixture of Cu-Zn-Al and/or Cu-Zn-Al-M and γ-Al_2O_3 after exposure to the syngas mixture (used catalysts) are shown in Fig. 3. The CuO peaks in the fresh calcined form disappeared after exposure to the syngas mixture and metallic Cu [ICDD: 85-1326] became the main phase of copper and ZnO remains unchanged. However, diffraction lines due to ZnO in the used form are predominant and broad when compared to the fresh calcined samples (Fig. 2), where poorly crystalline peaks are observed. The reflections attributed to γ-Al_2O_3 [ICDD: 47-1308] peaks in minor intensity could be seen over the used catalysts.

3.2. SEM-EDS and TPR

The SEM pictures of the calcined Cu-Zn-Al and Cu-Zn-Al-M (M = Ga, La, Y, Zr) catalysts are shown in Fig. 4. The elemental compositions of Cu, Zn, Al, Ga, La, Y and Zr obtained from the EDS analyses are presented in Table 1. It is observed that the compositions

Table 3
Surface compositions of Cu, Zn, Al, M (M = Ga, La, Y and Zr) atomic % excluding carbon content.

Catalyst	Cu	Zn	Al	O	M	Cu/Zn	Cu/Al	Zn/Al
CZA	19.8	12.7	10.8	56.7	–	1.56	1.83	1.17
CZAGa	17.0	12.3	9.7	59.5	1.5	1.37	1.75	1.27
CZALa	17.8	11.9	11.8	57.3	1.2	1.50	1.51	1.00
CZAY	20.2	10.5	12.8	55.4	1.1	1.93	1.57	0.81
CZAZr	20.0	15.1	10.8	52.2	1.9	1.33	1.86	1.40

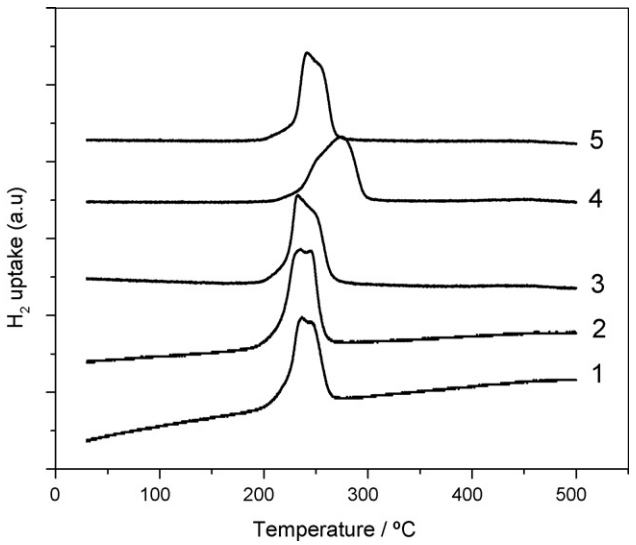

Fig. 5. TPR patterns of the calcined (1) Cu-Zn-Al-Y, (2) Cu-Zn-Al-Zr, (3) Cu-Zn-Al-La, (4) Cu-Zn-Al-Ga and (5) Cu-Zn-Al catalysts.

determined by chemical analysis are in close agreement with the nominal compositions taken for the catalysts preparations. SEM micrographs of the samples reveal that the particles are of uniform shape almost spherical in all the samples but the particles sizes are different. At least 50 particles have been chosen in order to measure the average particle size of the catalysts. The structural changes in Cu/ZnO catalysts are studied by Grunwaldt et al. [17] who found that the morphology of copper particles are found to be disk-like on the partially reduced ZnO surface, while on the fully oxidized ZnO surface the copper particles became more spherical in shape due to the weak interaction between copper and ZnO [17]. Fig. 3 evidently shows that the Cu-Zn-Al-Ga sample forms larger particles than Cu-Zn-Al, Cu-Zn-Al-La, Cu-Zn-Al-Y and Cu-Zn-Al-Zr catalysts. The average particle sizes of the samples are presented in Table 2. The H_2-TPR of the calcined samples is performed up to 500 °C at a ramping rate of 10 °C/min and the corresponding profiles are illustrated in Fig. 5. A broad reduction profile with a shoulder peak observed, which obviously consists of two-stage reduction. It appears that almost complete CuO reduction took place below 270 °C over all the samples except for the Cu-Zn-Al-Ga catalyst, where the T_{max} shifted to higher temperatures. The reduction peak centered at 235 °C is due to reduction of Cu^{2+} interacting with the alumina matrix and the shoulder peak appeared at 260 °C may be attributed to the stepwise reduction of copper oxide ($Cu^{2+} \rightarrow Cu^{+} \rightarrow Cu^{0}$) which could indicate a strong interaction between part of the copper and ZnO in the sample. Robinson and Mol observed a similar phenomenon in the TPR analysis of Cu-Zn-Al catalysts [18]. Iamarino et al. found that reduction of Cu^{2+} on the Al_2O_3 matrix occurs at 200 °C and that the bulk $CuAl_2O_4$ reduction takes place at high temperatures [19]. Therefore, it can be suggested that part of copper interacts with Al_2O_3 and some parts of copper with ZnO particles. The Cu-Zn-Al-Ga catalyst showed unusual reduction profile compared to the other catalysts wherein the T_{max} is observed at 275 °C. The shift in T_{max} towards high temperatures suggests a bulk CuO nature over the Cu-Zn-Al-Ga catalyst. SEM analysis shows that Cu-Zn-Al-Ga has average particle size of ca. 100 nm, supporting the formation of large CuO crystallites over the other catalysts, which is in good agreement with TPR analysis and N_2O titration.

3.3. N_2O decomposition and XPS analysis

The Cu metal surface areas are measured by N_2O titration and the corresponding values are presented in Table 2. The lowest Cu metal surface area of ca. 1.4 m^2/g is found with the Cu-Zn-Al-Ga catalyst and the higher copper metal surface area of about ca. 11.7 m^2/g is observed over the Cu-Zn-Al-Y catalyst. It appears that the yttrium modification enriched the copper on the catalyst surface.

The XPS analysis results corresponding to the Cu 2p, Zn 2p, Al 2p and O1s core-level spectra are displayed in Fig. 6a–d, respectively and the elemental surface compositions are presented in Table 3. All the spectra are referenced to C 1s located at 284.6 eV. The Cu $2p_{3/2}$ core-level peak shown in Fig. 6a is located at BE of 932.7 eV, except for the Cu-Zn-Al-Ga sample, where BE is slightly shifted to 933.2 eV and a strong shaking peak centered at 941.0 eV appeared in all the samples suggesting the presence of Cu^{2+} state, according to the standard XPS data [20] for CuO. The Zn $2p_{3/2}$ peak at 1021.7 eV can be assigned to Zn^{2+} species (Fig. 6b) on the catalyst surface. The deconvolved spectra of Al 2p are represented in Fig. 6c. It shows that the Al 2p peak can be clearly distinguished from the Cu $3p_{3/2}$ and Cu $3p_{1/2}$ peaks. The Al 2p peak centered at BE of 73.1 eV could be seen over Cu-Zn-Al, Cu-Zn-Al-La and Cu-Zn-Al-Y catalysts whereas there is a slight shift in BE found with Cu-Zn-Al-Ga and Cu-Zn-Al-Zr catalysts. In contrast, the Cu $3p_{3/2}$ peak appeared at a BE of 76.4 eV over all the modified catalysts except the unmodified Cu-Zn-Al catalyst which displayed a peak at 75.6 eV. Finally it can be concluded that upon deconvolution using the Gaussian peak fitting procedure the Al 2p and Cu $3p_{3/2}$, Cu $3p_{1/2}$ peaks are clearly visualized and distinguished. The O1s peaks in ternary compounds and mixed complex metal oxide catalysts are deconvolved and resolved with the Gaussian peak-fitting procedure (Fig. 6d). The O1s peaks in CuO, ZnO and Al_2O_3 phase are observed at the binding energy of 529.6, 531.2 and 531.8 eV respectively, which are in agreement with literature [20–22]. The O1s core-level peak (Fig. 6d), assigned to CuO, is shifted to lower binding energies, i.e. 527.8, 528.2, 529.2, and 528.4 eV over Cu-Zn-Al, Cu-Zn-Al-La, Cu-Zn-Al-Zr and Cu-Zn-Al-Y, respectively. However, the O1s peak due to CuO in the Cu-Zn-Al-Ga catalyst is observed at 529.7 eV. No appreciable peak shift is found due to O1s in ZnO and Al_2O_3.

EDS analysis of the bulk compositions has revealed that the Cu/Zn ratio is higher than unity and quite similar to those (Table 3) obtained from XPS analysis. The average particle size of ca. 54.7 nm over the Cu-Zn-Al-Y catalyst implies that copper is highly dispersed on catalyst surface, which is also evidenced from the high copper metal surface area over the other catalysts. The Cu/Al ratios are not much changed with the addition of Ga, La, Y and Zr into Cu-Zn-Al, but the Cu/Zn ratios are changed. From this observation it can be concluded that addition of small amounts of metal cation drastically modifies the surface copper/zinc compositions. Furthermore, Cu/Zn = 1.92 (Table 3) over Cu-Zn-Al-Y catalyst indicates that yttrium addition can enrich the surface Cu content on CuO/ZnO particles.

3.4. Activity studies

The temperature dependence of CO conversion, DME and CH_3OH yields are presented in Fig. 7a–c. The Cu-Zn-Al-M catalysts are physically mixed with γ-Al_2O_3 before the reaction. The CO conversion increases with an increase in the reaction temperature and the highest activity is observed over the Cu-Zn-Al-Y catalysts admixed with γ-Al_2O_3 throughout the temperature region of 250–280 °C compared to other catalysts. It should be mentioned here that the selectivity towards DME is almost constant (~68%) and that the methanol yields are found to be below 2%. No hydrocarbon by-products are observed. The differences in the CO conversion between CZA and Cu-Zn-Al-Y decreased with an increase in the reaction temperature, because the CO conversion is approaching the equilibrium conversion. Therefore, the activity comparison between the catalysts would be meaningful at the low reaction temperature. From this point of view, the CO conversions over the

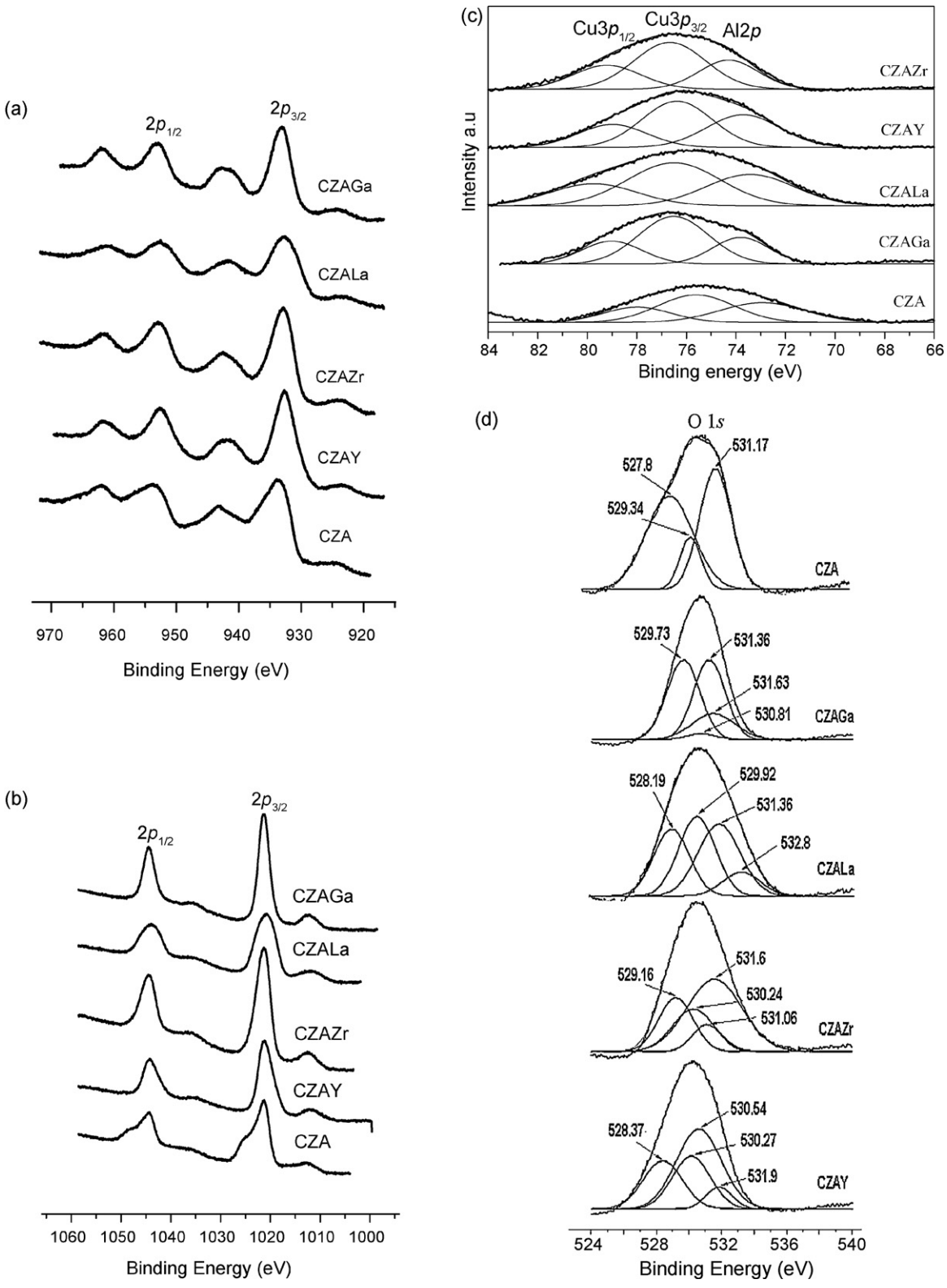

Fig. 6. The XPS core-level spectra of Cu2p (a), Zn2p (b), Al2p (c) and O1s (d) of the Cu-Zn-Al and Cu-Zn-Al-M (M = Ga, La, Y, and Zr) catalysts.

Cu-Zn-Al and Cu-Zn-Al-M catalysts admixed with γ-Al_2O_3 against their Cu metal surface areas at 250 °C are presented in Fig. 8. It appears that the reaction rates with the admixed catalysts are proportional to Cu metal surface area of the Cu-Zn-Al-M catalysts. Catalysts with high Cu metal surface lead to high CO conversions and consequently higher DME yields. The gallium promoted CZA shows reasonably good activity although the copper metal surface area is very low. Except gallium, the La-, Y- and Zr-modified Cu-Zn-Al catalysts admixed with γ-Al_2O_3 have a similar turnover number based on Cu surface areas as observed in Fig. 8. In terms of the turnover rate based on Cu surface areas, Cu-Zn-Al-Ga seems to be a better catalyst over the other catalysts. However, high copper

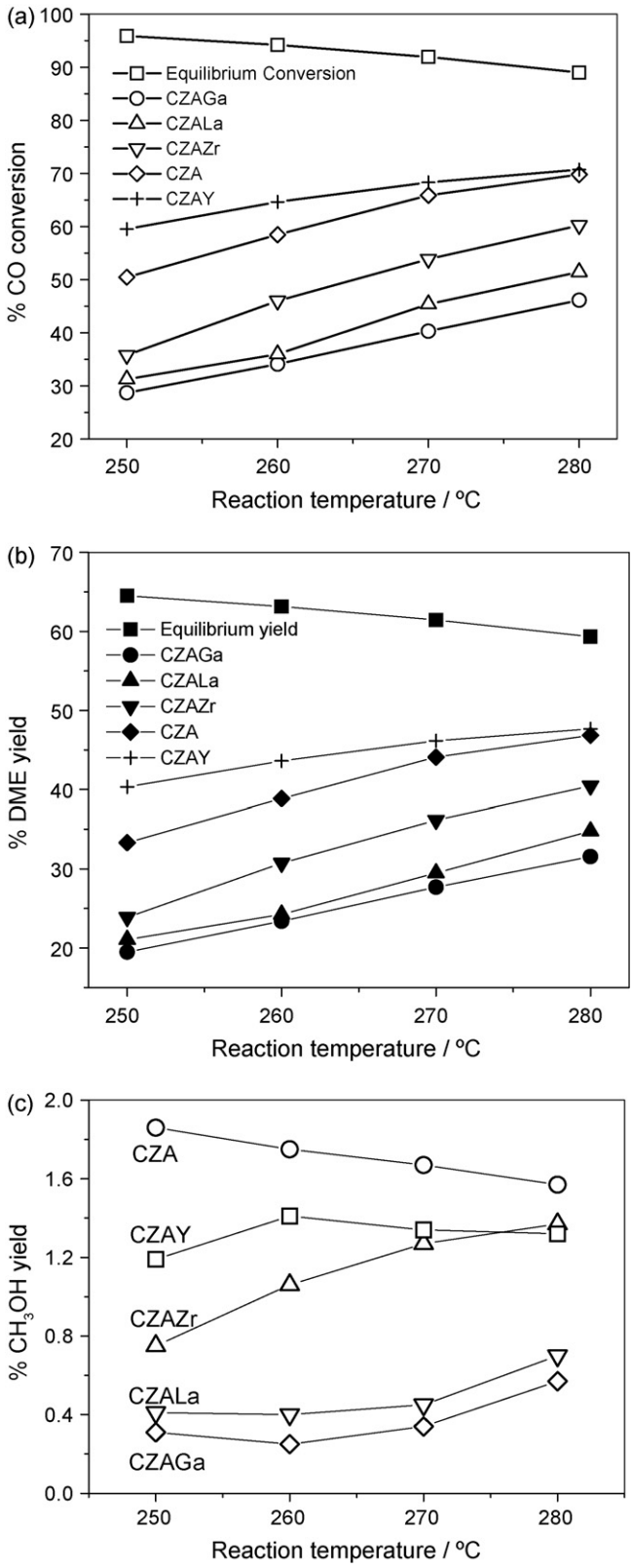

Fig. 7. The temperature dependence on the CO conversion (a), DME yield (b) and CH_3OH yields (c) over Cu-Zn-Al and Cu-Zn-Al-M (M = Ga, La, Y and Zr) catalysts admixed with γ-Al_2O_3: GHSV = 6000 h^{-1}, H_2/CO = 1.5, pressure = 600 psig.

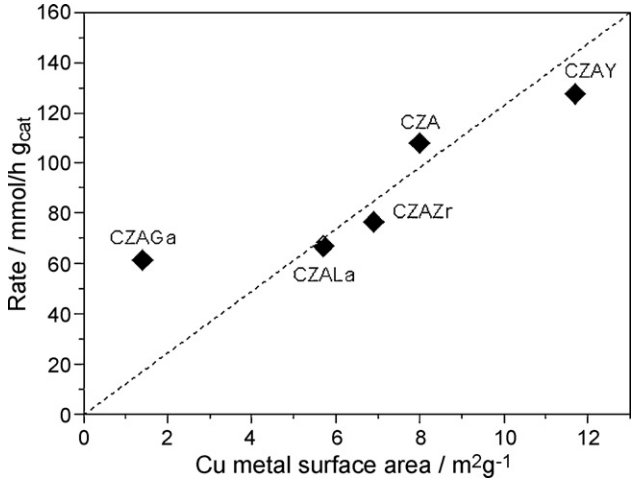

Fig. 8. Copper metal surface areas of Cu-Zn-Al and Cu-Zn-Al-M (M = Ga, La, Y and Zr) catalysts *vs.* reaction rates on the admixed catalysts with γ-Al_2O_3 at 250 °C, H_2/CO = 3/2, pressure 600 psig and GHSV = 6000 h^{-1}.

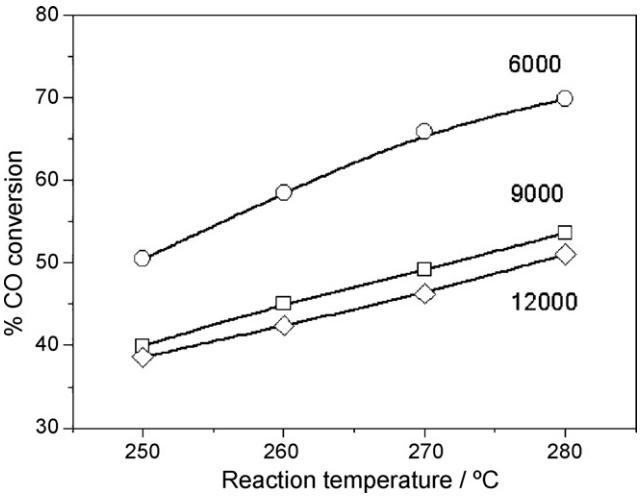

Fig. 9. CO conversion at GHSV ranged from 6000 to 12,000 h^{-1} over Cu-Zn-Al-Y catalysts admixed with γ-Al_2O_3: pressure 600 psig and H_2/CO ratio 3/2.

surface area is an important factor in order to achieve higher syngas conversions and higher CO conversions.

Yttrium is an element with high oxygen affinity as well as a tendency to inhibit the copper particle grain growth even up to 580 °C [23]. Probably this could be the reason why Cu-Zn-Al-Y sample displayed high specific surface area of 113.5 m^2/g and also the higher copper metal surface area of 11.7 m^2/g. The effect of GHSV on CO conversion and the DME yields with the Cu-Zn-Al-Y catalyst at different gas hourly space velocities from 6000 to 12,000 h^{-1} in a range close to industrial conditions is studied and the results are presented in Fig. 9. The CO conversions decreased with an increase in GHSV. However, at a high GHSV of 12,000 h^{-1} and the temperature of 280 °C the CO conversions and the DME yields are very high as compared to other catalysts [6,24].

4. Conclusions

Precursors of Cu-Zn-Al and Cu-Zn-Al-M (M = Ga, La, Y and Zr) hydrotalcite-like structures produced finely dispersed copper particles upon thermal decomposition in air at 400 °C. Yttrium-modified Cu-Zn-Al showed BET-surface areas higher than the other modified and unmodified catalysts. The activity of the admixed catalysts of Y-modified Cu-Zn-Al and γ-Al_2O_3 is superior to the other cat-

alysts in the temperature range of 250–280 °C. The Ga-, La- and Zr-modified Cu-Zn-Al catalysts admixed with γ-Al_2O_3 showed the activity lower than the unmodified Cu-Zn-Al, which is explained by the low copper metal surface area. Small amounts of yttrium addition dramatically increased Cu metal surface areas, resulting in the high CO conversion and DME yields even at a high GHSV of 12,000 h^{-1}. Finally the high copper dispersion over Cu-Zn-Al-Y is explained by the inhibition of copper particle grain growth induced by yttrium which is evidenced from high BET-surface area, N_2O titration studies and small particle size revealed by SEM analysis.

Acknowledgments

This work is financially supported by a program of Energy and Resources Technology Development. One of the authors A.V.G. acknowledges the KOFST (Korea) for financial support, Director-IICT, Hyderabad and CSIR-New Delhi for approval to visit KIST.

References

[1] A.C. Sofianos, M.S. Scurrell, Ind. Eng. Chem. Res. 30 (1991) 2372.
[2] Q. Ge, Y. Huang, F. Qiu, S. Li, Appl. Catal. A: Gen. 167 (1998) 23.
[3] L.-L. Li, X.-G. Zhang, T. Inui, Appl. Catal. A: Gen. 147 (1996) 23.
[4] S. Lee, M.R. Gogate, C.J. Kulik, Chem. Eng. Sci. 47 (13–14) (1992) 3769.
[5] T. Takeguchi, K. Yanagisawa, T. Inui, M. Inoue, Appl. Catal. A: Gen. 192 (2000) 201.
[6] J.H. Kim, M. Park, O.S. Joo, K.D. Jung, Appl. Catal. A: Gen. 264 (2004) 37.
[7] F.S. Ramos, A.M. Duarte de Farias, L.E.P. Borges, J.L. Monteiro, M.A. Fraga, E.F. Sousa-Aguiar, L.G. Appel, Catal. Today 101 (2005) 39.
[8] R.H. Hoppener, E.B.M. Doesburg, J.J.F. Scholten, Appl. Catal. A: Gen. 25 (1986) 109.
[9] C. Busetto, G.D. Piero, G. Manara, J. Catal. 85 (1984) 260.
[10] R.L. Frost, Z. Ding, W.N. Martens, T.E. Johnson, Thermochim. Acta 398 (2003) 167.
[11] B. Peplinski, W.E.S. Unger, Appl. Surf. Sci. 62 (1992) 115.
[12] J. Nakamura, Y. Choi, T. Fujitani, Topics Catal. 22 (2003) 277.
[13] Hong-Bo Chen, Dai-Wei Liao, La-Jia Yu, Yi-Ji Lin, J. Yi, Hong-Bin Zhang, Khi-Rui Tsai, Appl. Surf. Sci. 147 (1999) 85.
[14] J.W. Evans, M.S. Wainwright, A.J. Bridgewater, D.J. Young, Appl. Catal. 7 (1983) 75.
[15] F. Trifiro, A. Vaccari, G.D. Piero, in: K.K. Unger, J. Raoquerol, K.S.W. Sing, H. Kral (Eds.), Characterization of Porous Solids, Elsevier, Amsterdam, 1988, p. 571.
[16] W.R.A.M. Robinson, J.C. Mol, Appl. Catal. A: Gen. 60 (1990) 61.
[17] J.-D. Grunwaldt, A.M. Molenbroek, N.-Y. Topsoe, H. Topsoe, B.C. Clausen, J. Catal. 194 (2000) 452.
[18] W.R.A.M. Robinson, J.C. Mol, Appl. Catal. A: Gen. 76 (1991) 129.
[19] M. Iamarino, R. Chirone, L. Lisi, R. Pirone, P. Salatino, G. Russo, Catal. Today 75 (2002) 317.
[20] J.F. Moulder, W.F. Sickle, P.E. Sobol, K.D. Bomben, in: J. Chastain (Ed.), Handbook of Photoelectron Spectroscopy, PerkinElmer C. Physical Electronics Division, USA, 1992.
[21] C. Battistoni, J.L. Dormann, D. Fiorani, E. Paparazzo, S. Viticoli, Solid State Commun. 39 (1981) 581.
[22] R.T. Figueiredo, A. Martinez-Arias, M. Lopez Granados, J.L.G. Fierro, J. Catal. 178 (1998) 146.
[23] Dirk Weiss, Ph D Thesis: Deformation Mechanisms in Pure and Alloyed Copper Films, Max-Planck-Instiut fur Metallforschung und Institut fur Metallkunde der Universitaet, Stuttgart, 2000.
[24] Akula Venugopal, Jelliarko Palgunadi, Oh-Shim Joo, Jung Kwang Deog, 2006, Filed Korean Patent, Catalyst development: process for preparing precursors of catalysts containing copper, zinc, yttrium, aluminum, for the synthesis of DME from syngas, and references therein.